SUPPLEMENTARY NOTE 3: LU-HF ANALYSIS OF THE ITSAQ AND ACASTA GNEISS COMPLEXES

Geological and sample descriptions

The Itsaq Gneiss Complex

The IGB is located within Western Greenland and consists primarily of 3.9-3.7 Ga TTG gneisses[152,153]. During this time interval, various TTG intrusive stages occurred, many of which were also associated with the emplacements of felsic volcanic rocks, basalts and komatiites, and tectonic intercalation of these various units. Assembly of the IGC units occurred at c. 3.65 Ga, which is when magmatism switched to becoming dominated by crust-derived granites and Fe-Ti gabbros, and regional metamorphism commenced[153]. Peak conditions for this metamorphism are estimated at c. 580 °C and 0.65 GPa[154]. These Itsaq gneisses contain fragmented supracrustal belts of the Akilia formation and the Isua Greenstone belt (IGB)[155]. The IGB comprises amphibolite, with subordinate amounts of BIF, metachert, dolostone, and other metasedimentary rocks[156]. The Akilia Formation, which occurs on Akilia Island south of the IGB, consists of amphibolite gneiss, ultramafic rocks, BIF, metasedimentary rocks, mafic dykes (the Ameralik dykes), and leucocratic granitoids (Bridgwater & McGregor, 1974; Manning, 2006). The protoliths of the formation and ISB largely formed between 3.8-3.7 Ga[155,157-159], and were metamorphosed to conditions reaching up to the granulite facies. The IGB was subjected to regional metamorphism at c. 2.71 Ga and regional granite magmatism at 2.55 Ga[127,154,160-162]. The sample analyzed in this study (*SM/GR00/23*; Fig. S1) is an amphibolite sampled in the IGC just south of the Isua core complex. The sample consists primarily of hornblende, quartz, clinopyroxene, garnet, and plagioclase, with trace tourmaline, orthoclase, ilmenite, apatite and titanite, and minor secondary epidote and calcite. The sample shows a weak foliation defined by the shape-preferred orientation of hornblende. Garnet ($alm_{61-63}prp_{17-19}grs_{17-18}sps_{2-3}$) occurs as sub- to euhedral porphyroblasts of 2-5 mm in diameter and contains minor inclusions of phases that make up the primary assemblage. Plagioclase is bytownite to labradorite (an_{67-80})

Acasta Gneiss Complex

The AGC is located along the western fringe of the Slave Craton, within the northwestern portion of the Canadian Shield. The Slave Craton consists of four major units, the Central Slave Basement Complex (CSBC; >2.9 Ga)[163], the Central Slave Cover Group (2.9-2.8 Ga)[164-166], the supracrustal rocks of the Yellowknife Supergroup (2.72-2.65 Ga)[167,168], and younger tonalitic to granitic syn- to post-tectonic plutons (2.62-2.58 Ga)[169]. The CSBC consists of deformed and heterogeneous TTG and biotite-hornblende orthogneiss interlayered with amphibolitized mafic intrusions and subordinate amounts of calc-silicate gneiss, quartzite, biotite schist and ultramafic schist[164-166,169]. The CSBC is split into east and west regions by a north-east trending fault, with felsic gneiss occurring predominantly in the eastern domain and layered gneiss being common in the western domain. Peak metamorphic *P-T* conditions for the AGC, which crops out in the western domain of CSBC, are estimated at c. 750 °C and 0.45-0.62 GPa, and these conditions are indicate to have occurred sometime in the late Archean[129]. The basement rocks of the CSBC are overlain by the Central Slave Cover Group (CSCG), which primarily consists of Cr-rich BIF and quartzite, as well as tholeiitic and calc-alkaline basalts. The Yellowknife Supergroup is uncomfortably deposited on top of the CSCG and consists of pillow basalts and intermediate felsic volcanic rocks overlain by turbidites and polymict conglomerates. The sample analyzed in this study (*BNB-95-103*; Fig. S2) is from the AGC, which crops out in the western domain of CSBC. The sample is a garnet-bearing amphibolite sampled along the Acasta River just east of the fault that transects the CSBC. The sample comprises hornblende, quartz and plagioclase with minor garnet, biotite, and iron

oxides (Figure 7a-f). Garnet ($alm_{52-64}prp_{2-4}grs_{20-32}sps_{12-16}$) occurs as relatively large (up to 1 cm), subhedral porphyroblasts that contain all phases listed above as inclusions.

Analytical methods

The grain with the largest cross-sectional area found in this section was selected for major-element analysis by electron probe micro-analyzer (EPMA) and REE analysis by laser ablation inductively coupled plasma mass spectrometry (LA-ICPMS). Major-element spot analysis and mapping was done by wavelength-dispersive spectroscopy using a JEOL Ltd. *JXA-iHP200F* field-emission EPMA operating at 20 nA and 15 kV at the Electron Microbeam and X-ray Diffraction Facility (EMXDF) at the Department of Earth, Ocean and Atmospheric Sciences (EOAS), University of British Columbia (UBC), Canada. The k_α X-ray lines of Mn, Fe, Ti and Cr (LIFL), K and Ca (PETL), Na and Mg (TAPL), and Si and Al (TAP) were analyzed applying on- and off-peak counting time was 20 seconds and linear baseline corrections. The analyses were calibrated against natural albite (Na and Si), corundum (Al), pyrope (Mg), orthoclase (K), spessartine (Mn), chromite (Cr), diopside (Ca), hematite (Fe), and rutile (Ti). For mapping, the intensities of k_α X-ray lines of Fe, Mg, Ca, Mn, and Cr were analyzed using crystals TAPL, LILF, PETL, LIFL, and PETL, respectively. Relevant compositional results are included in the sample description in Supplementary Note 2. The major-element maps for Fe, Mg, Ca and Mn are provided in Supplementary Figures S1 and S2 (Cr showed no resolvable zoning in the samples).

Garnet REE compositions were determined by LA-ICPMS using an Resonetics *RESOlution M-50-LR* excimer LA system coupled to an Agilent *7700x* single-quadrupole ICPMS at the Pacific Centre for Isotopic and Geochemical Research (PCIGR), EOAS-UBC. The grains subjected to major-element analysis were analyzed in thin section along the paths shown in the maps above. Analytical spots were staggered along the paths, avoiding inclusions, cracks and other irregularities. Grains were ablated for 40 s using a spot-size of 47 μm, a repetition rate of 8 Hz and a laser energy of 100 mJ. Internal normalization was done by measuring m/z corresponding to ^{29}Si, using average Si concentrations measured in each grain by EPMA. External normalization was done by repeat bracketing analyses of the NIST 612 reference between every 8 unknown analyses. The *BCR-2G* basalt glass reference was analyzed to evaluate accuracy. Measured concentrations match known concentrations within the precision of the analyses (Supplementary Table S2).

Garnet Lu-Hf analyses were Garnet separates and bulk-rock powders were analyzed for isotope dilution Lu-Hf geochronology at the Pacific Centre for Isotopic and Geochemical Research (PCIGR), University of British Columbia, Vancouver, Canada. Garnet separates were handpicked under a binocular microscope. Whole-rock separates were prepared by taking small intact pieces of rock and crushing these by hand using an agate mortar and pestle. Garnet separates were bathed in dilute (1N) HCl at room temperature, before being washed twice with de-ionized water, weighed, and spiked with a ^{176}Lu-^{180}Hf isotope tracer solution. The garnet sample-spike mixtures for garnet were dissolved at atmospheric pressure by the alternate addition of HF, HNO_3, $HClO_4$, and 6 N HCl, with solution drying down between each step. Spiked whole-rock powders were dissolved using a standard high-pressure digestion approach to ensure congruent dissolution; they were digested in HF-HNO_3 kept at 180 °C in a stainless-steel autoclave digestion vessel for 7 days. The Lu-Hf isotope analyses were conducted using a Nu Instruments Ltd. *Plasma I* multi-collector inductively coupled plasma mass spectrometry instrument. The Lu and Hf isobaric interference corrections were done following Blichert-Toft et al.[170]. The Hf isotope ratios were normalized to ATI-475, which is made from and is isotopically identical to JMC-475 ($^{176}Hf/^{177}Hf = 0.282160$[171]). The external reproducibility of ATI-475 $^{176}Hf/^{177}Hf$ measured at sample equivalent concentrations was 23 ppm. External reproducibility of unknown $^{176}Hf/^{177}Hf$ was estimated on the basis of

analytical error and the relation between error (1 %RSE) and reproducibility (2 %RSD) as calibrated through repeat analyses of ATI-475 at concentrations that bracket those of the unknowns[172]. Isochron regressions and age calculations were done using Isoplot v. 4.15[173], applying a λ^{176}Lu value[174-175] of 1.867 $\times 10^{-11}$ yr^{-1}. The isotope and age data are presented in Supplementary Table S3 and shown as part of Supplementary Figures S1 and S2.

Supplementary Table S2: REE data obtained for the BCR-2G reference material by LA-ICPMS

REE	Concentration (ppm)	Concentration (ppm)[1]
La	25.5 ± 0.8	24.73
Ce	53.9 ± 1.7	53.3
Pr	6.72 ± 0.33	6.77
Nd	28.3 ± 1.8	28.87
Sm	6.68 ± 0.43	6.588
Eu	1.98 ± 0.13	1.965
Gd	6.55 ± 0.42	6.712
Tb	1.01 ± 0.06	1.1
Dy	6.43 ± 0.34	6.437
Ho	1.31 ± 0.08	1.28
Er	3.68 ± 0.22	3.697
Tm	0.503 ± 0.05	0.532
Yb	3.47 ± 0.28	3.391
Lu	0.506 ± 0.052	0.503

[1] Jochum et al. (2005)

Results

Garnet major- and trace-element compositions

Garnet from *SM/GR/0023* (IGC) shows a clear core-and-rim relationship, with concentric zoning of decreasing Ca and Mn, and increasing Ca towards the rims (Fig. S1). Manganese and, to a lesser extent, Ca are enriched in the outermost rims. Calcium shows flame-type zoning toward the rim. Garnet in all samples shows concentric REE zoning, with a HREE-enriched core (*BNB-14-066A*) and/or several HREE-enriched annuli. Given the absence of volumetrically significant HREE-enriched cores in all samples, the Lu-Hf ages – if at all significantly weighed to a certain zone – would be weighed towards the age of garnet located in the outer 50% radial distance from grain cores.

Garnet in *BNB-95-103* (AGC) shows complex major-element zoning, with a general rim-ward decreasing Fe and Mg concentrations, and increasing Mn concentrations, as well as an intervening network of microstructures that are depleted in Fe and Mg, and enriched in Ca (Fig. S2). Zoning for Mn is smooth and follows the grain shape, indicating diffusive relaxation. These microstructures segment the analyzed grain into smaller microdomains with garnet habit and locally show trains of inclusions. It is possible that these microstructures represent sealed cracks or sub-grain walls. Garnet in *BNB-14-066A* (NGB) does not show strong zoning. The analyzed grain shows a broad core-and-rim texture with high Mn and Mg in the core and high Fe and Ca in the rims. At east for Mg, zoning follows the anhedral grain shape indicating diffusive relaxation.

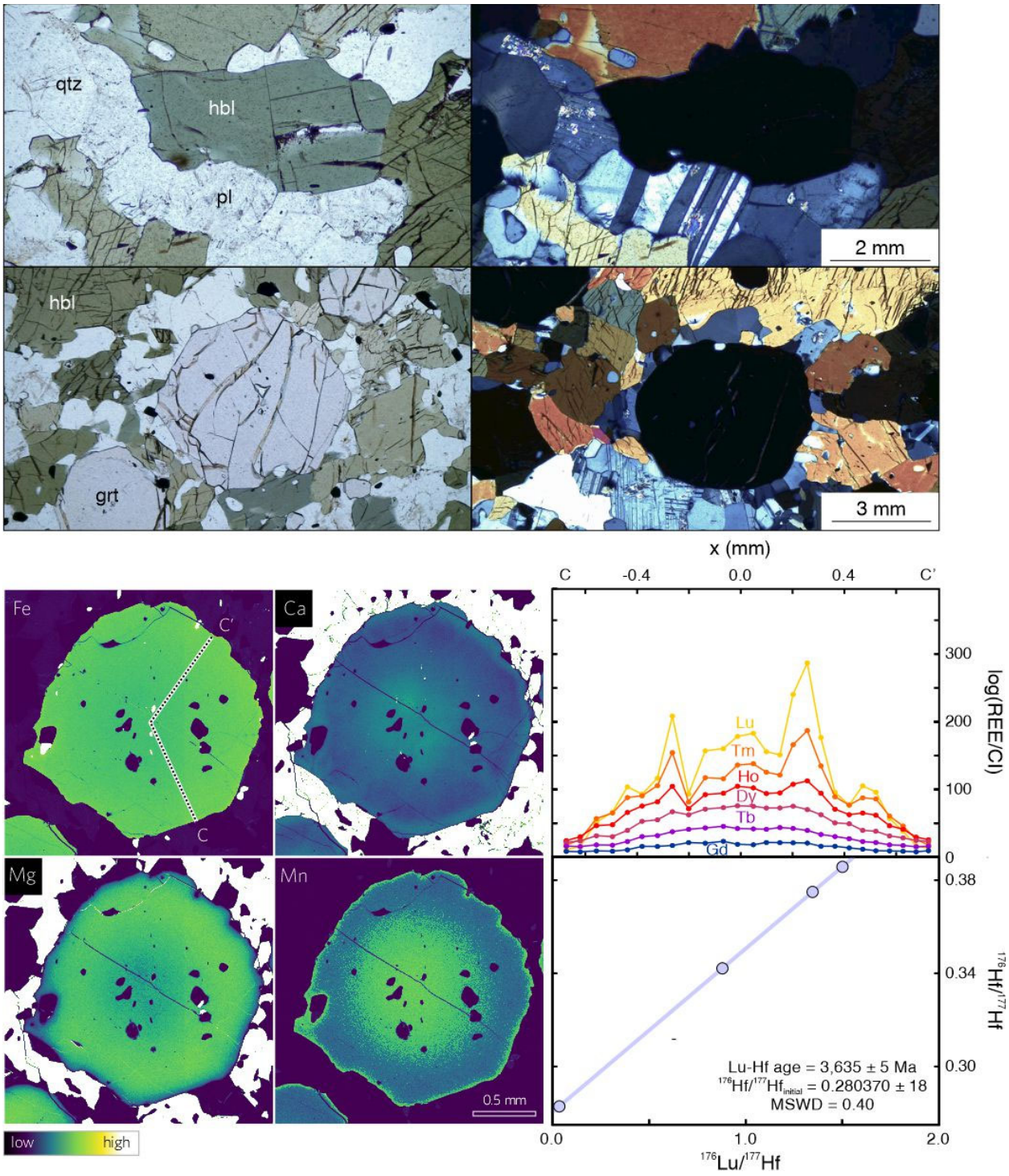

Supplementary Fig. S1: Photomicrographs and analytical results for the IGC amphibolite sample *SM/GR00/23*. Mineral abbreviations: hbl – hornblende; pl – plagioclase; grt – garnet; qtz – quartz.

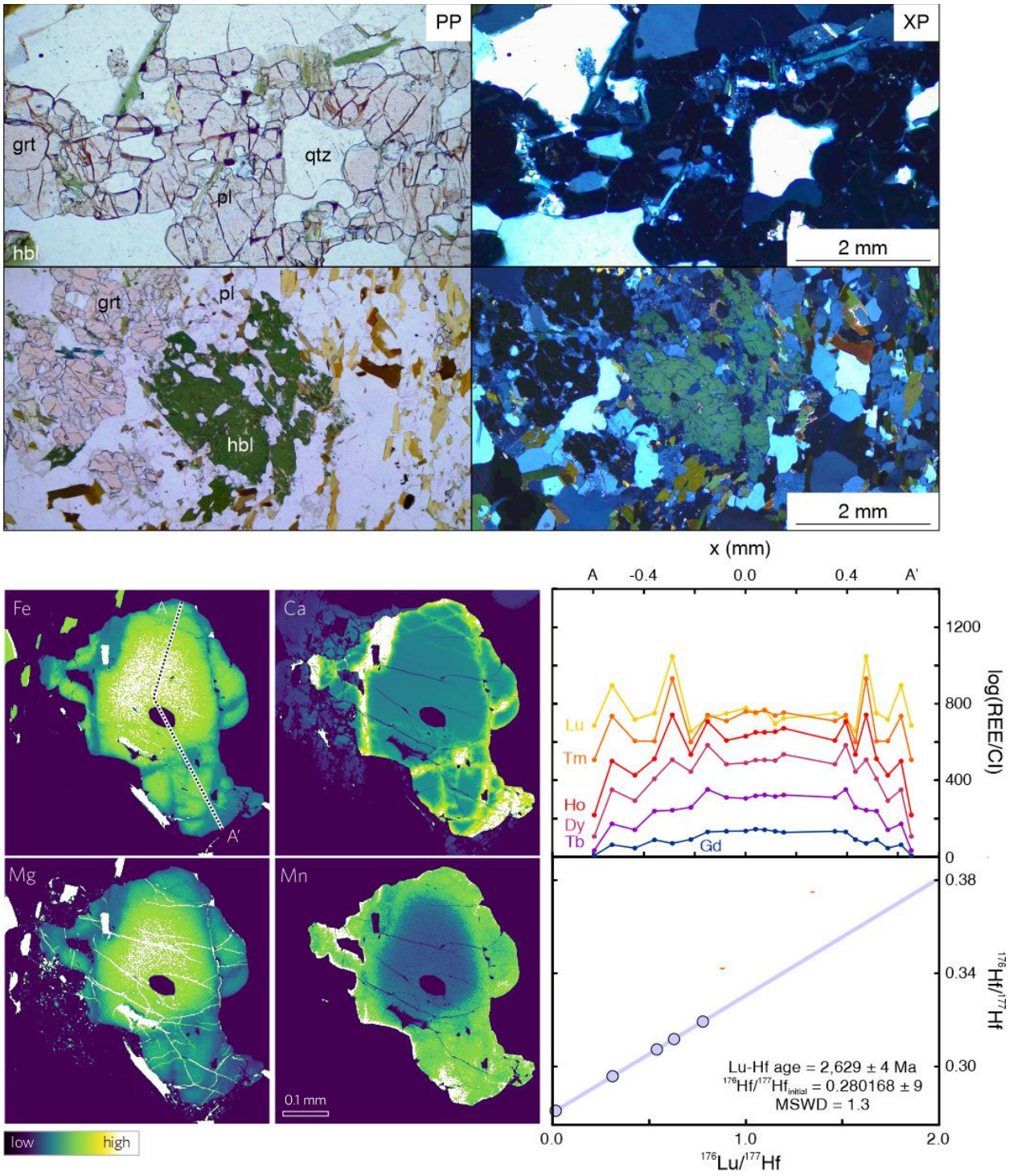

Supplementary Figure S2: Photomicrographs and analytical results for the AGC amphibolite sample *BNB-95-103*. Mineral abbreviations: hbl – hornblende; pl – plagioclase; grt – garnet; qtz – quartz.

Garnet Lu-Hf age results

Garnet in the IGB amphibolite *SM/GR/0023* provided a Lu-Hf age of 3,635 ± 5 Ma (n = 4; MSWD = 0.56; $^{176}Hf/^{177}Hf_i$ = 0.280370 ± 0.000018; Fig. S1). The initial $^{176}Hf/^{177}Hf$ value for this isochron is indistinguishable from chondritic at the age of garnet growth, indicating the protolith was formed from such reservoir at the time of garnet growth or was extracted from a depleted reservoir a few 100 Myr prior. The Lu-Hf age broadly resembles c. 3.7-Ga Sm-Nd dates obtained from amphibolites sampled in the amphibolite unit fringing the Isua dome just north of the *SM/GR/0023* sample location (Blichert-Toft & Frei, 2001) and is similar to 3.65-Ga $^{207}Pb/^{206}Pb$ ages of obtained from zircon overgrowths in diorite gneisses on Akilia Island in the SW IGC (Whitehouse et al., 1999). The age of c. 3.64 Ga marks the transition from TTG, to gabbro- and granite magmatism and represents the onset of regional low-*P* metamorphism and shearing across the IGC[153]. A much younger Lu-Hf age was obtained from flattened garnet porphyroclasts in a metapelitic schist from the western ISB (2,551 ± 74 Ma)[127]. The latter was suggested to preclude Eoarchean metamorphism of the ISB, which is hereby disproven. Resembling the c. 2.6-Ga $^{207}Pb/^{206}Pb$ ages of rare zircon tips in various TTG gneisses[152], this Lu-Hf age likely dates renewed metamorphism associated with the tectonic reworking of the ISB in the Neoarchean.

Garnet in AGC amphibolite *BNB-95-103* provided a Lu-Hf age of 2,629 ± 4 Ma (n = 5; MSWD = 1.3; $^{176}Hf/^{177}Hf_i$ = 0.280168 ± 0.000009; Fig. S2). The initial $^{176}Hf/^{177}Hf$ values would indicate crustal model ages of 4.2-4.0 Ga, which are consistent with the age of the oldest crust found in these terranes[176]. The Lu-Hf garnet age for the AGC amphibolite matches the main stage of deformation and metamorphism associated with the assembly of the Slave Craton (2.62-2.60 Ga)[177]. The Lu-Hf age also confirms the age of 2,661 ± 22 Ma identified among a range of garnet dates obtained from in-situ Lu-Hf analysis[129].

Supplementary Table S3: Lu-Hf data for the analyzed samples.

Sample	Lu (ppm)	Hf (ppm)	$^{176}Lu/^{177}Hf$	$^{176}Hf/^{177}Hf$	Lu-Hf age	$^{176}Hf/^{177}Hf_{initial}$	MSWD
BNB-95-103 (Acasta Gneiss Complex)							
Grt-1	26.1	6.86	0.5388 ± 13	0.307282 ± 17			
Grt-2	23.7	4.33	0.7771 ± 19	0.319257 ± 20			
Grt-3	29.4	6.65	0.6280 ± 16	0.311704 ± 17			
Grt-4	27.5	12.6	0.3102 ± 8	0.295804 ± 16			
WR-1	1.01	9.04	0.01575 ± 4	0.280960 ± 9			
					2629 ± 4 Ma	**0.280168 ± 9**	**1.3**
SM/GR/0023 (Itsaq Gneiss Complex)							
Grt-1	3.17	0.511	0.8788 ± 22	0.342094 ± 19			
Grt-2	4.24	0.401	1.500 ± 3	0.385652 ± 23			
Grt-3	3.88	0.409	1.345 ± 3	0.374893 ± 18			
WR-1	0.379	1.54	0.03498 ± 9	0.282827 ± 16			
					3635 ± 5 Ma	**0.280370 ± 18**	**0.40**

Uncertainties are 2 s.d. in the last significant digits of the mean. WR = autoclave-digested whole-rock powder.

References (not in main text)

[152] Whitehouse, M.J., Kamber, B.S. & Moorbath, S. Age significance of U–Th–Pb zircon data from early Archaean rocks of west Greenland—a reassessment based on combined ion-microprobe and imaging studies. *Chemical Geology* **160**, 201–224 (1999).

[153] Nutman, A.P. *et al.* The Itsaq Gneiss Complex of Greenland: Episodic 3900 to 3660 Ma juvenile crust formation and recycling in the 3660 to 3600 Ma Isukasian orogeny. *American Journal of Science* **313**, 877–911 (2013).

[154] Ramírez-Salazar, A. *et al.* Tectonics of the Isua Supracrustal Belt 1: P-T-X-d Constraints of a Poly-Metamorphic Terrane. *Tectonics* **40**, (2021).

[155] Nutman, A.P., McGregor, V.R., Friend, C.R.L., Bennett, V.C. & Kinny, P.D. The Itsaq Gneiss Complex of southern West Greenland; the world's most extensive record of early crustal evolution (3900-3600 Ma). *Precambrian Research* **78**, 1–39 (1996).
[156] Bridgwater, D. & McGregor, V.R. Field work on the very early Precambrian rocks of the Isua area, southern West Greenland. *Rapport Grønlands Geologiske Undersøgelse* **65**, 49–54 (1974).
[157] Moorbath, S., O'Nions, R.K. & Pankhurst, R.J. Early Archaean Age for the Isua Iron Formation, West Greenland. *Nature* **245**, 138–139 (1973).
[158] Crowley, J. L. U–Pb geochronology of 3810–3630 Ma granitoid rocks south of the Isua greenstone belt, southern West Greenland. *Precambrian Research* **126**, 235–257 (2003).
[159] Kamber, B., Whitehouse, M.J., Bolhar, R. & Moorbath, S. Volcanic resurfacing and the early terrestrial crust: Zircon U–Pb and REE constraints from the Isua Greenstone Belt, southern West Greenland. *Earth and Planetary Science Letters* **240**, 276–290 (2005).
[160] Rollinson, H. The metamorphic history of the Isua Greenstone Belt, West Greenland. *Geological Society, London, Special Publications* **199**, 329–350 (2002).
[161] Rollinson, H. Metamorphic history suggested by garnet-growth chronologies in the Isua Greenstone Belt, West Greenland. *Precambrian Research* **126**, 181–196 (2003).
[162] Næraa, T. *et al.* Hafnium isotope evidence for a transition in the dynamics of continental growth 3.2 Gyr ago. *Nature***485**, 627–630 (2012).
[163] O'Neil, J., Carlson, R.W., Paquette, J.-L. & Francis, D. Formation age and metamorphic history of the Nuvvuagittuq Greenstone Belt. *Precambrian Research* **220–221**, 23–44 (2012).
[164] Bleeker, W., Ketchum, J. W. & Davis, W.J. The Central Slave Basement Complex, Part II: age and tectonic significance of high-strain zones along the basement-cover contact. *Canadian Journal of Earth Sciences* **36**, 1111–1130 (1999).
[165] Sircombe, K.N., Bleeker, W. & Stern, R.A. Detrital zircon geochronology and grain-size analysis of a ~2800 Ma Mesoarchean proto-cratonic cover succession, Slave Province, Canada. *Earth and Planetary Science Letters* **189**, 207–220 (2001).
[166] Ketchum, J.W.F., Bleeker, W. & Stern, R.A. Evolution of an Archean basement complex and its autochthonous cover, southern Slave Province, Canada. *Precambrian Research* **135**, 149–176 (2004).
[167] Helmstaedt, H. & Padgham, W.A. A new look at the stratigraphy of the Yellowknife Supergroup at Yellowknife, N.W.T. — implications for the age of gold-bearing shear zones and Archean basin evolution. *Canadian Journal of Earth Sciences* **23**, 454–475 (1986).
[168] Jenner, G.A., Fryer, B. J. & McLennan, S.M. Geochemistry of the Archean Yellowknife Supergroup. *Geochimica et Cosmochimica Acta* **45**, 1111–1129 (1981).
[169] Iizuka, T. *et al.* Geology and zircon geochronology of the Acasta Gneiss Complex, northwestern Canada: New constraints on its tectonothermal history. *Precambrian Research* **153**, 179–208 (2007).
[170] Blichert-Toft, J., Boyet, M., Télouk, P. & Albarède, F. ^{147}Sm–^{143}Nd and ^{176}Lu–^{176}Hf in eucrites and the differentiation of the HED parent body. *Earth and Planetary Science Letters* **204**, 167–181 (2002).
[171] Vervoort, J.D. & Blichert-Toft, J. Evolution of the depleted mantle: Hf isotope evidence from juvenile rocks through time. *Geochimica et Cosmochimica Acta* **63**, 533–556 (1999).
[172] Bizzarro, M., Baker, J. A., Haack, H., Ulfbeck, D. & Rosing, M. Early history of Earth's crust–mantle system inferred from hafnium isotopes in chondrites. *Nature* **421**, 931–933 (2003).
[173] Ludwing, K.R. ISOPLOT 3.75 a Geochronological Toolkit for Microsoft Excel. *Berkeley Geochronology Centre Special Publication* **5**, 1-75 (2012)
[174] Scherer, E.E., Münker, C. & Mezger, K. Calibration of the Lutetium-Hafnium Clock. *Science* **293**, 683–687 (2001).
[175] Söderlund, U., Patchett, P.J., Vervoort, J.D. & Isachsen, C.E. The ^{176}Lu decay constant determined by Lu–Hf and U–Pb isotope systematics of Precambrian mafic intrusions. *Earth and Planetary Science Letters* **219**, 311–324 (2004).

[176] Reimink, J.R., Chacko, T., Stern, R.A. & Heaman, L.M. The birth of a cratonic nucleus: Lithogeochemical evolution of the 4.02–2.94 Ga Acasta Gneiss Complex. *Precambrian Research* **281**, 453–472 (2016).
[177] Isachsen, C.E. & Bowring, S.A. Evolution of the Slave craton. *Geology* **22**, 917 (1994).